24th INTERNATIONAL CONGRESS ON SOUND AND VIBRATION
23–27 July 2017, London

DYNAMIC RESPONSE OF TWO-STATE HYDROMOUNTS WITH TWIN INERTIA TRACKS

Judith Picken

University of Southampton, Institute of Sound and Vibration Research, Highfield, Southampton, UK, & Tun Abdul Razak Research Centre, Brickendonbury, Hertford, UK
email: jpicken@tarrc.co.uk

David Thompson and Stephen Daley

University of Southampton, Institute of Sound and Vibration Research, Highfield, Southampton, UK,

The paper considers adaptive hydromounts for automotive engines. Conventional hydromounts typically contain a single inertia track tuned to the resonance frequency of the mass of the engine on the mounts. The paper describes an adaptive mount with two inertia tracks, one of which can be switched on or off. This enables the mount to be tuned to a second resonance frequency and is only operational when required, for instance to control the transmission of engine vibrations to the vehicle during idling. An experimental rig that allows aspects of the geometrical design of the mount to be altered has been used to investigate the role of various parameters on the dynamic response of the twin track mount. Experimental dynamic response data across a range of frequencies with different inertia track characteristics is presented. Moreover, a linear model for the twin track adaptive hydromount is proposed, and the initial values for the parameters of the model are determined. The model is then verified against the experimental data and the parameters of the model are optimised to fit the data. The implications of the change from the initial to the optimum values are then considered.
Keywords: adaptive hydromount, inertia track, two-state engine mount, dynamic behaviour

1. Introduction

The design of passive engine mounts involves managing a compromise between two or more conflicting requirements. On one hand, for effective isolation of the cabin from engine vibrations, generated by the movement of engine parts during ignition cycles, the mount is required to be as soft as possible. However, when the vehicle is travelling on rough road surfaces, a soft mounting system would lead to large engine block movements occurring at the natural frequency of the engine mounting system. These large amplitude, low frequency oscillations of the engine block are perceived as inferior ride quality.

Hydromounts are passive components consisting of a conventional soft spring in parallel with a tuned-mass-damper. The tuned-mass-damper part of the mount is designed to coincide with the natural frequency of the engine mounting system. The tuned-mass-damper consists of the compliances of the two chambers and an inertia track connecting them. Under certain circumstances it is beneficial to have a second tuned frequency; for example, to control the transmission of engine vibrations to the vehicle during idling. A second resonance frequency can be provided by the addition of a secondary inertia track connecting the primary chamber to a third compliant chamber.

This paper considers a linear model for such a mount, together with a means of estimating the chamber compliance. This is compared with experimental results and updated values for the compliance are derived. The implications of this are discussed.

2. Theoretical considerations

2.1 Model for the twin-track hydromount

A diagram of the model for a twin-track hydromount can be seen in Fig. 1. The mount consists of three chambers. Chambers 2 and 3 are connected through two separate inertia tracks to chamber 1.

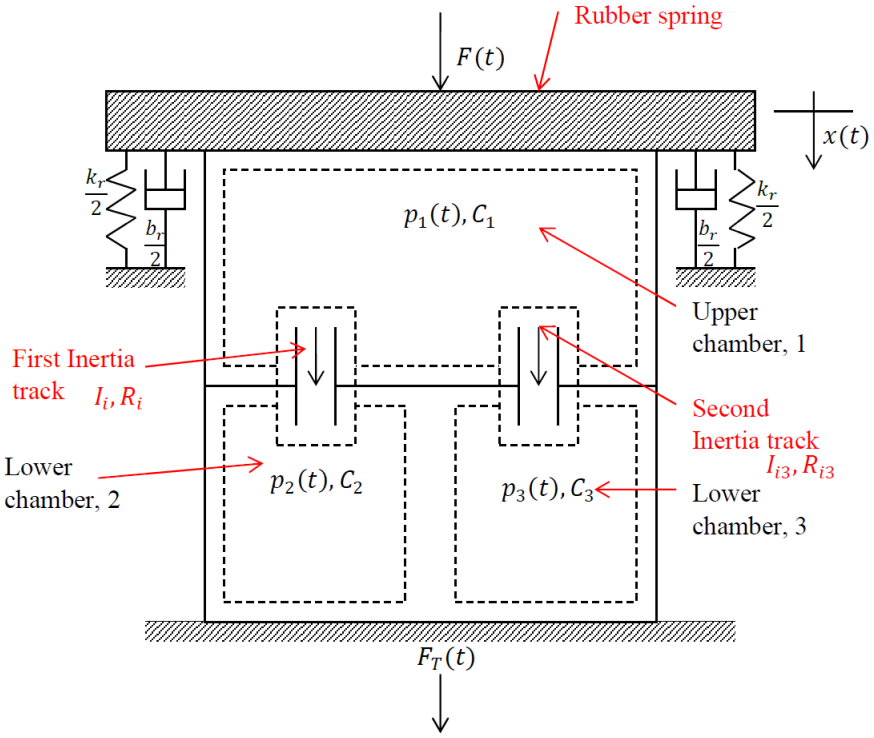

Figure 1: Diagram representing fluid model of hydromount

From the equations of motion for the system an expression for a linear model can be obtained in a similar way to the one-track hydromount described by Singh *et al.*[1].

$$K^*(\omega) = \frac{F_T(\omega)}{x(\omega)} = \frac{i\alpha_5\omega^5 + \alpha_4\omega^4 - i\alpha_3\omega^3 - \alpha_2\omega^2 + i\alpha_1\omega + \alpha_0}{\beta_4\omega^4 - i\beta_3\omega^3 - \beta_2\omega^2 + i\beta_1\omega + \beta_0} \tag{1}$$

where

$$\alpha_5 = b_r I_i I_{i3} C_1 C_2 C_3,$$
$$\alpha_4 = b_r C_1 C_2 C_3 (I_i R_{i3} + I_{i3} R_i) + (k_r C_1 + A_r^2) C_2 C_3 I_i I_{i3},$$
$$\alpha_3 = b_r C_1 (C_3 I_{i3} + C_2 I_i + C_2 C_3 R_i R_{i3}) + b_r C_3 C_2 I_i + b_r C_2 C_3 I_{i3} + C_2 C_3 (k_r C_1 + A_r^2)(I_i R_{i3} + I_{i3} R_i),$$
$$\alpha_2 = b_r C_1 (R_i C_2 + R_i C_3) + b_r C_2 C_3 (R_i + R_{i3}) + (k_r C_1 + A_r^2)(I_{i3} C_3 + I_i C_2 + R_i C_2 R_{i3} C_3) + k_r C_2 C_3 (I_i + I_{i3}),$$
$$\alpha_1 = b_r (C_1 + C_2 + C_3) + k_r C_1 + A_r^2 (R_i C_2 + R_{i3} C_3) + k_r C_2 C_3 (R_i + R_{i3}),$$
$$\alpha_0 = k_r (C_1 + C_2 + C_3) + A_r^2,$$
$$\beta_4 = C_1 C_2 C_3 I_i I_{i3},$$
$$\beta_3 = C_1 C_2 C_3 (I_i R_{i3} + I_{i3} R_i),$$
$$\beta_2 = C_1 (I_{i3} C_3 + I_i C_2 + C_2 C_3 R_i R_{i3}) + C_2 C_3 (I_i + I_{i3}),$$

$$\beta_1 = C_1(R_iC_2 + R_{i3}C_3) + C_2C_3(R_i + R_{i3}),$$
$$\beta_0 = C_1 + C_2 + C_3$$

where F_T is the force transmitted through mount, x is the displacement of the mount, b_r is the damping coefficient of the rubber spring, k_r is the stiffness of the rubber spring, A_r is the surface area of the rubber spring, C_1, C_2 and C_3 are the compliances of the chambers 1, 2 and 3 respectively, I_i and I_{i3} are the inertances of inertia tracks 1 and 2 respectively, R_i and R_{i3} are the fluid resistances of inertia tracks 1 and 2 respectively.

2.2 Compliance of the chambers

The volumetric compliances of the chambers are crucial in defining the resonance frequencies of the mount. For this system the compliance of the first chamber is dependent on the rubber spring and an annular rubber diaphragm within the chamber. The compliances of the other two chambers are governed by the rubber diaphragms at the end of the chambers (not shown).

To model the compliances it is assumed that the diaphragms in chambers 2 and 3 are spherical caps and the material is neo-Hookean. From Rivlin's theory of large strain elasticity [2] the compliance ($C = \Delta V/\Delta P$) of the cap is estimated from expressions for the volume and the pressure:

$$V_{\text{cap}} = \frac{\pi}{6}(3c^2 + h^2)h \tag{2}$$

$$P_{\text{cap}} = \frac{4hGt_0}{c^2 + h^2}(1 - \lambda_1^{-6}) \tag{3}$$

where c is the radius of the uninflated diaphragm, h is the height of the spherical cap, G is the shear modulus of the rubber, t_0 is the thickness of the rubber and λ_1 is the principal extension ratio.

The annular diaphragm of chamber 1 is treated similarly but with the shape being a cap on a cylinder, leading to the following expressions for the volume and the pressure:

$$V_{\text{capcyl}} = 2\pi d\left(\frac{\theta(c^2 + h^2)^2}{4h^2} - \frac{c(c^2 + h^2)}{2h} + ch\right) \tag{4}$$

$$P_{\text{cap}} = \frac{4hGt_0}{c^2 + h^2}(1 - \lambda_2^{-4}) \tag{5}$$

where d is the radius to the centre of the annulus, $\theta = \arcsin(2ch/(c^2 + h^2))$ and λ_2 is the principal extension ratio.

The compliance decreases with increasing pressure until it becomes almost constant, before ultimately rising again. The values of compliance chosen initially were from the constant compliance region.

The rubber spring has a more complex shape and so data from an FEA model in MARC was used. The rubber was modelled to be neo-Hookean with a shear modulus of 0.5MPa. This was added to the compliance of the annular ring to give the compliance of chamber 1. The calculated compliances for all the chambers can be seen in Fig. 2 (the various configurations will be described below).

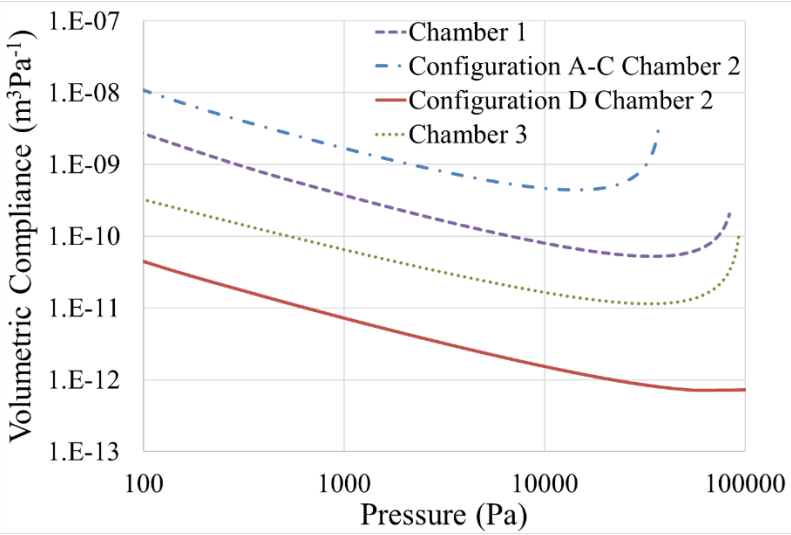

Figure 2: Calculated volumetric compliance of the three chambers

3. Experimental procedure

For testing the model a hydromount simulation rig was used. The second inertia track and the compliance for chamber 2 at the end of the first inertia track were adjustable and a number of different configurations were considered (Table 1). In all configurations the first inertia track had a length of 300mm and a diameter of 12.5mm, the compliances of chamber 1 and chamber 3 were estimated to be 7.51×10^{-11}m^{3}Pa^{-1} and 1.44×10^{-11}m^{3}Pa^{-1}. A preload of 1000N was applied and the testing was carried out on a VH7 Schenck servohydraulic machine at an amplitude of 0.1mm at 1Hz intervals over the frequency range 1-100Hz. A Solartron frequency response analyser was used to calculate complex dynamic stiffness from the displacement and force output channels.

Table 1: Configurations of the mount

Configuration	Length - Inertia Track 2 (mm)	Diameter - Inertia Track 2 (mm)	Compliance - Chamber 2 (m^{3}Pa^{-1})
A	12	7.5	5.34×10^{-10}
B	25	5	5.34×10^{-10}
C	170	20	5.34×10^{-10}
D	170	20	2.51×10^{-12}

4. Results

4.1 Comparison of the model with experiment

The initial results for the four configurations are shown in Figs. 3-6. As the linear model does not predict the magnitude of the dynamic stiffness well, discussion of these results mainly focuses on the shape of the curves and the location of the first two resonance frequencies of the mount. The initial results for configurations A, B and C (Figs. 3-5) showed reasonable agreement with the measurements in terms of the first resonance, but the second resonance was not correctly predicted, especially for A and C. For configuration D (Fig. 6), the general shape of the curves was reasonable, but both resonance frequencies were poorly predicted.

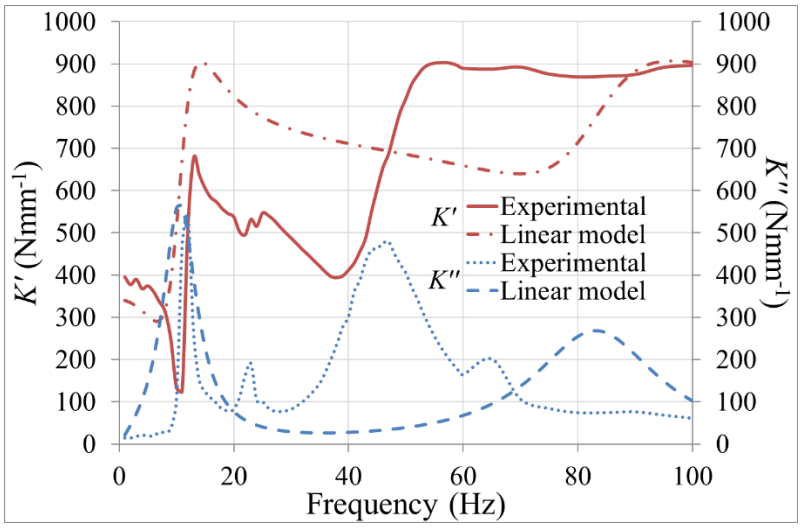

Figure 3: Results for Configuration A

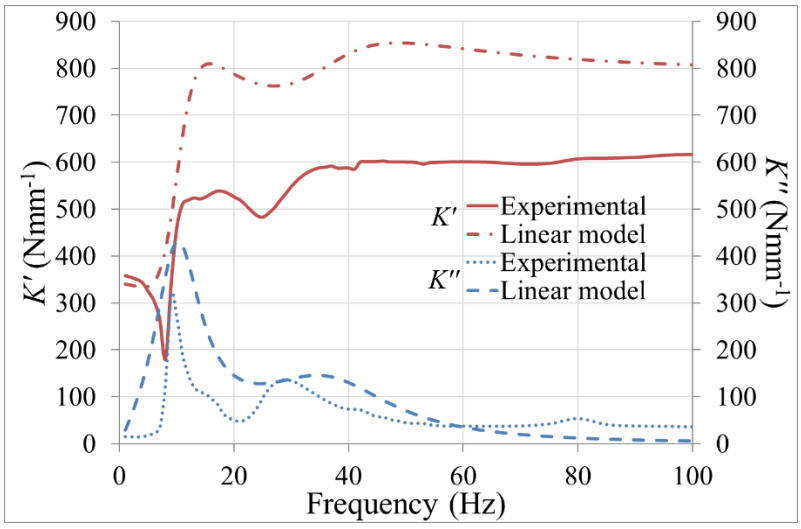

Figure 4: Results for Configuration B

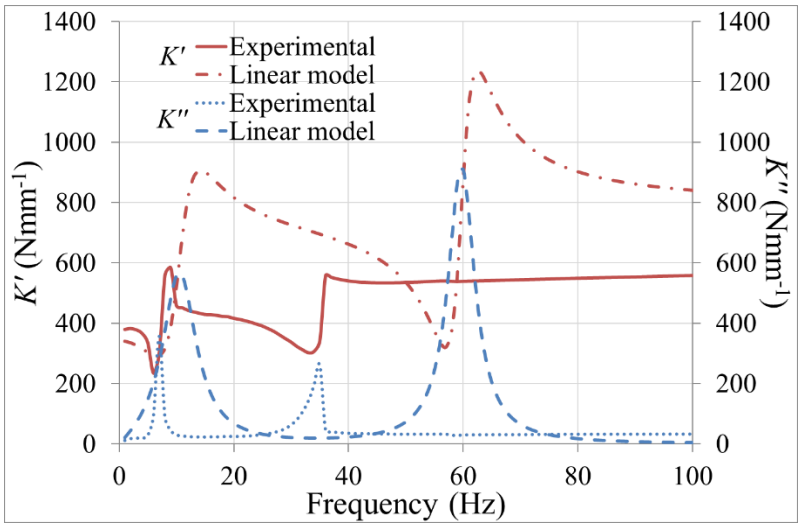

Figure 5: Results for Configuration C

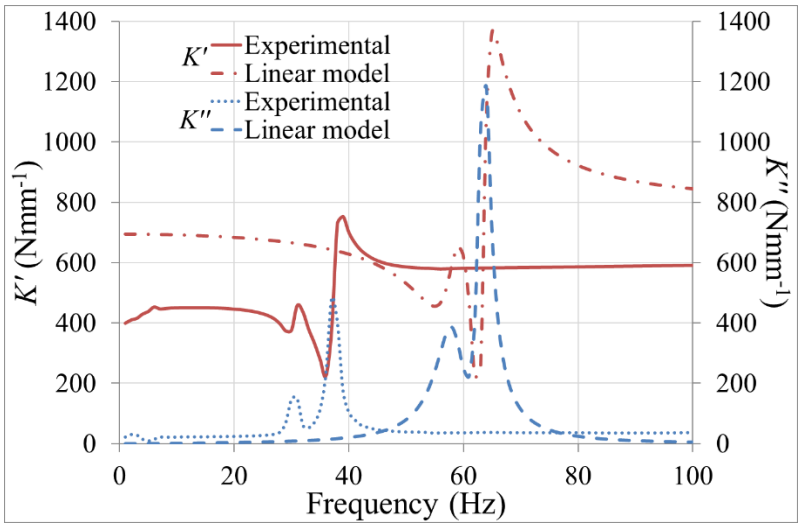

Figure 6: Results for Configuration D

4.2 Optimisation of the compliance

The resonance frequencies are very sensitive to the compliance of all three chambers as the values are so close in magnitude. The compliances were manually optimised to choose values that gave a good fit for the resonance frequencies. The new response curves can be seen in Figs. 7-10.

To obtain these improved curves, the compliances were altered to the values given in Table 2. The compliances for chambers 1 and 3, and also for chamber 2 in configuration D, are significantly softer than the initial values chosen. This could mean that the pressure within the chamber was either significantly higher or lower than that chosen initially. However for configurations A-C the compliance was overestimated. The method of predicting the compliance assumes the spherical cap is not inflated beyond a hemisphere. At this point a spherical cap is no longer a reasonable model for the shape of the diaphragm. If the pressures are significantly higher than those in Fig. 2 then this method of predicting the compliance is not valid.

To estimate the likely pressure in the chambers a time domain model (not discussed in this paper), with a harmonic input, was used including the new values for the compliances. The data was taken between 1 and 50Hz in 1 Hz intervals. The model does not consider the pressure applied by the preload.

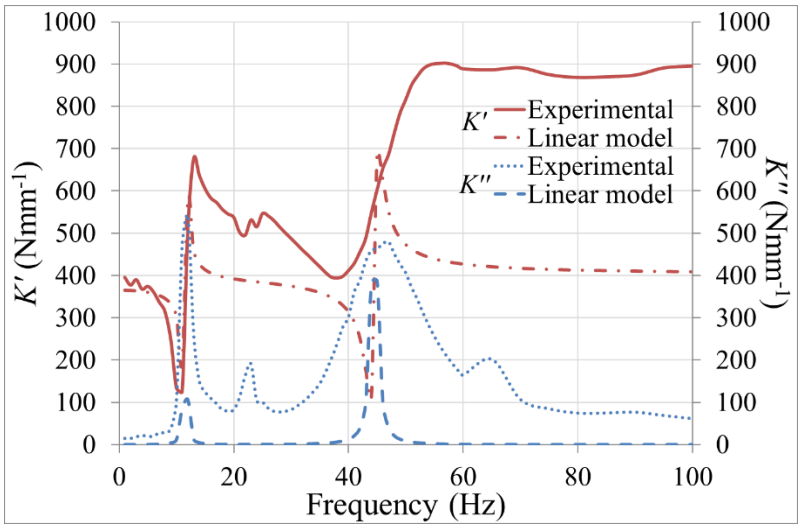

Figure 7: Improved results for Configuration A

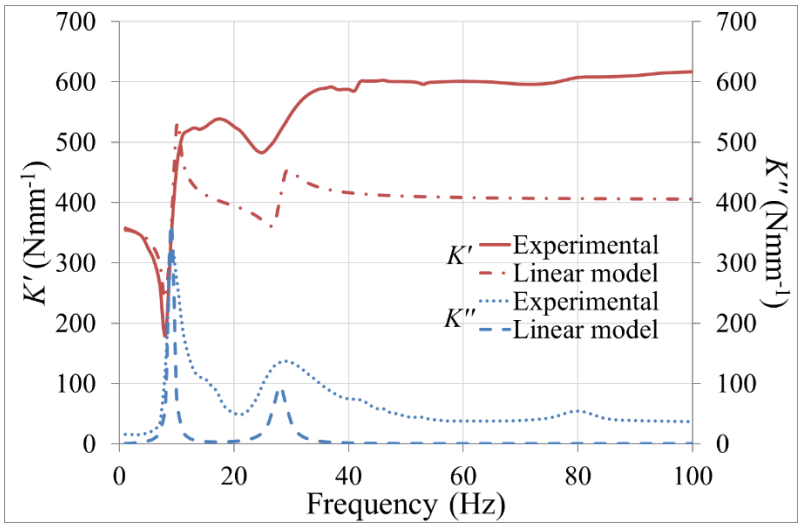

Figure 8: Improved results for Configuration B

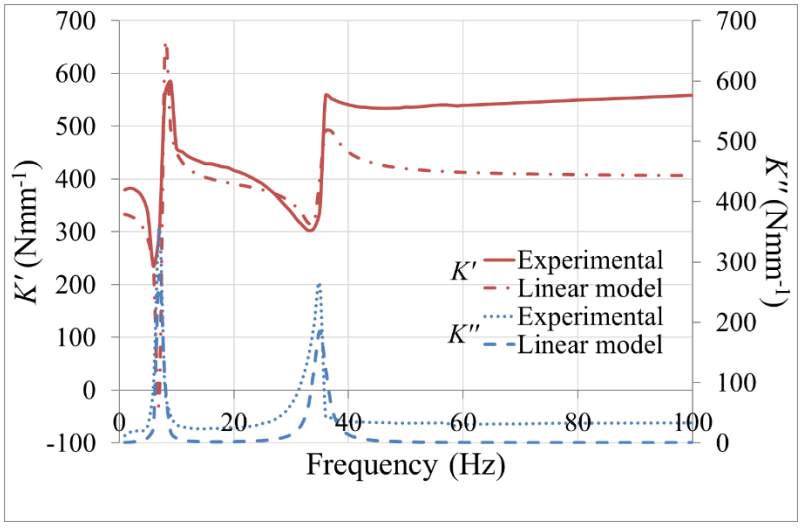

Figure 9: Improved results for Configuration C

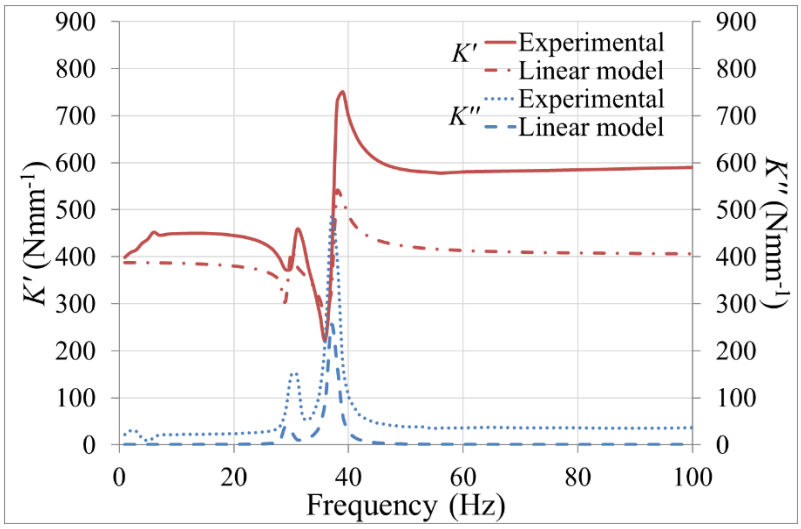

Figure 10: Improved results for Configuration D

Looking first at chamber 1, at 0.1mm amplitude all the configurations have a similar peak value of pressure between 5 and 7.5kPa. These values are significantly lower than those for which the initial compliance was a reasonable estimate. With reference to Fig. 2 the new value of 3.07×10^{-10} m^3Pa^{-1} seems to fit better with these pressure values.

Table 2: Compliances used in the model

Configuration	Compliance - Chamber 1 (m^3Pa^{-1})		Compliance - Chamber 2 (m^3Pa^{-1})		Compliance - Chamber 3 (m^3Pa^{-1})	
	Initial	Improved	Initial	Improved	Initial	Improved
A	7.51×10^{-11}	3.07×10^{-10}	5.34×10^{-10}	8.90×10^{-11}	1.44×10^{-11}	5.04×10^{-11}
B	7.51×10^{-11}	3.07×10^{-10}	5.34×10^{-10}	1.78×10^{-10}	1.44×10^{-11}	2.52×10^{-11}
C	7.51×10^{-11}	3.07×10^{-10}	5.34×10^{-10}	3.56×10^{-10}	1.44×10^{-11}	3.96×10^{-11}
D	7.51×10^{-11}	3.07×10^{-10}	2.51×10^{-12}	1.13×10^{-11}	1.44×10^{-11}	3.46×10^{-11}

For chamber 3, the peak pressures are approximately 6kPa, 8kPa, 55kPa and 55kPa for configurations A, B, C and D. For configurations A and B these values are lower than the flat portion of the curve in Fig. 2, and the compliances will be higher than the initial value. For configurations C and D the pressures are similar, as are the compliances. However, the pressure does not seem high enough to warrant the increase in the compliance between the initial values and the improved values. This may be because the peak values are missed as the peaks are sharp and the increments of 1Hz relatively coarse. If the peak pressure is higher the compliance could be in the high pressure upturn region observed in Fig. 2.

For chamber 2 there are two different set-ups. For configuration D the peak pressure was approximately 50kPa, but again the peak was quite sharp and may have been missed. The initial value seems in line with the pressure value. For configurations A, B and C the peak pressures were 16kPa, 13kPa and 7kPa respectively. Although the peaks were sharp, there is not a clear justification for the reduction in the compliance.

5. Conclusions

A linear model and a method for estimating compliance were proposed and the predictions of the model compared with experimental values. Initially the agreement was found to be poor, but adjusting the compliances gave a substantial improvement in fit. The adjustment in compliances appears justifiable when looking at the likely pressures in the chambers of the mounts. At high pressures the method of compliance prediction seems to underestimate the compliance. This is likely due to the shortcomings in the use of the spherical cap at high inflations, where the height of the cap is equal to or beyond that of a hemisphere.

Further work needs to be done to improve the estimation of the compliance at high pressures. Improving the time domain model to predict more accurately the pressure would also be of benefit. The added complication of any internal pressure applied by the preload should also be considered.

6. Acknowledgements

The authors would like to acknowledge Julia Gough of TARRC for the FEA of the spring and Hamid Ahmadi of TARRC for his advice.

REFERENCES

1 Singh, R., Kim, G., Ravindra, P. V. Linear analysis of automotive hydro-mechanical mount with emphasis on decoupler characteristics, 1992 *Journal of Sound and Vibration,* **158**, 219-243, (1992).

2 Treloar L. R. G. *The physics of rubber elasticity*, 3rd Edition, Clarendon Press, Oxford (1975).